

Bifurcation Control for Mitigating Subsynchronous Oscillations in Power Systems

A. M. Harb¹

A. H. Nayfeh²

L. Mili¹

¹Bradley Department of Electrical and Computer Engineering

²Department of Engineering Science and Mechanics

Virginia Polytechnic Institute and State University

Blacksburg, VA 24061

Abstract – A bifurcation control is proposed to mitigate subsynchronous oscillations of the CHOLLA # 4 turbine-generator system with respect to the SAGUARO station through a capacitor-compensated transmission line. The system is operated by the Arizona Public Service Company. Unlike the studies reported in the literature, the present bifurcation analysis is carried out on a complete model that accounts for machine saturation, damper windings, and the dynamics of the automatic voltage regulator (AVR). To increase the compensation level and thereby augment the transfer capability of the line, a power system stabilizer has been designed and added to the AVR. Because the stability region is load dependent, a nonlinear controller that acts on the excitation system is also proposed to significantly reduce the amplitudes of the torsional oscillations.

Keywords: Subsynchronous resonance, bifurcation analysis, nonlinear control.

1 - INTRODUCTION

In their work carried out during the Navajo project, Farmer *et al.* [1] identified three types of subsynchronous resonance (SSR): transient torque effect, induction generator effect, and torsional interaction effect. Unlike the last two effects, transient torques are not self-excited. They are rather induced by system disturbances that tend to excite the natural modes of the turbine-generator masses, which cause them to oscillate relative to one another.

By contrast, the induction generator effect [2, 3] is caused by self-excitation of the synchronous generators. It occurs when the resistance of the rotor to the subsynchronous current, viewed from the armature terminal, becomes negative and exceeds in magnitude the positive resistance of the network at the natural frequencies. As a result, subsynchronous currents and torques will sustain themselves, which in turn may damage the shaft of the machine. Another type of self-excited torque may build up due to the so-called torsional interaction effect. It occurs when the difference between the synchronous and natural subsynchronous frequencies is close to the natural frequency of a torsional mode of

the shaft.

Most of the techniques that are advocated in the literature to study SSR are frequency scanning, eigenvalue analysis, and EMTP [1-3]. The frequency scanning is particularly effective in the examination of the induction generator effect. Unfortunately, it cannot identify self-excited torsional oscillations. Another method to study this type of oscillations is eigenvalue analysis [4-6]. Because this approach is linear, it is appropriate to complement it by a nonlinear analysis to design controllers that are effective in damping nonlinear oscillations. One relevant theoretical framework for this analysis is provided by bifurcation theory.

The most commonly encountered bifurcation in power systems is the Hopf bifurcation [6]. It occurs when a complex conjugate pair of eigenvalues of the linearized model about the operating condition transversely crosses the imaginary axis of the complex plane [7]. This gives rise to the birth of limit cycles (i.e., isolated periodic solutions) from an equilibrium point. The existence of smoothly growing limit cycles as the capacitor compensation level μ increases was revealed by Mitani *et al.* [8], Zhu *et al.* [9], and Nayfeh *et al.* [10, 11]. In these studies, various simplifications of the machine model are assumed. In [8], the simplest model that can exhibit subsynchronous resonance is considered; it consists of a single turbine section coupled to a generator that has no damper windings and AVR and has a non-saturated magnetic circuit. A first improvement to the model is made in [9, 10] by considering a turbine with high-, intermediate-, and low-pressure sections. Further improvements are reported in [12], which consider a generator model with damper windings. Surprisingly, it is found that for these improved models, the instability occurs at a much lower level of capacitor compensation.

In this paper, we carry out a bifurcation analysis in a complete model of the CHOLLA # 4 turbine-generator system at the Arizona Public Service. The model considers machine saturation, damper windings, and the dynamics of the automatic voltage regulator (AVR). It neglects the turbine governor because its time constant is very large compared to those of the AVR's. The study shows that the

excitation system shrinks the stability region. To increase this region, we include a power system stabilizer (PSS) and tune it using bifurcation analysis. Because the stability region depends on the loadability of the system, a nonlinear controller is also proposed. It reduces significantly the amplitudes of the oscillations.

The paper is organized as follows. Section 2 outlines bifurcation and Floquet theories as applied to power systems. Section 3 describes the turbine-generator model, including saturation, damper windings, and AVR. Section 4 deals with the inclusion of a PSS to enlarge the stability region. In Section 5, we design a nonlinear controller to decrease the amplitude of the oscillations.

Notation: Underlined lower-case and upper-case letters denote a vector and a matrix, respectively. A star attached to a letter stands for its complex conjugate while an over dot indicates a time derivative.

2 - BIFURCATION ANALYSIS

Consider a nonlinear system governed by

$$\dot{\underline{X}} = \underline{F}(\underline{X}; \underline{m}) \quad (1)$$

where \underline{X} is a vector of n state variables, $\{x_1, x_2, \dots, x_n\}$, $\underline{F}(\cdot)$ is the field vector, and \underline{m} is the control parameter. The equilibrium points of the system satisfy the equation $\underline{F}(\underline{X}; \underline{m}) = \underline{0}$. Using a continuation method [7] (i.e., a pseudo-arclength scheme), this equation is solved as a function of \underline{m} to find the equilibrium points. To study the local stability of an equilibrium point \underline{X}_0 found at \underline{m}_0 , we apply to it a small disturbance \underline{y} . Then, we substitute $\underline{X}(t) = \underline{X}_0 + \underline{y}(t)$ into (1) to obtain $\dot{\underline{y}} = \underline{F}(\underline{X}_0 + \underline{y}; \underline{m})$. Finally, we apply a first-order Taylor series expansion about \underline{X}_0 , notice that $\underline{F}(\underline{X}_0; \underline{m}_0) = \underline{0}$, and obtain

$$\dot{\underline{y}} \approx \underline{J}(\underline{X}_0; \underline{m}_0) \underline{y} \quad (2)$$

where $\underline{J}(\underline{X}_0; \underline{m}_0) = \frac{\partial \underline{F}}{\partial \underline{x}}(\underline{X}_0; \underline{m}_0)$.

The local stability of \underline{X}_0 at \underline{m}_0 depends on whether all of the eigenvalues have negative real parts or not. In the former case, the equilibrium point is asymptotically stable. If the real parts of one or more eigenvalues are positive, the equilibrium is unstable.

2.1 Hopf Bifurcation

In the state-control space $(\underline{X}; \underline{m})$, we identify a stable equilibrium point $(\underline{X}_1; \underline{m}_1)$ and use a continuation scheme to find the loci of all the equilibrium points \underline{X} as \underline{m} is varied from \underline{m}_1 . These loci usually consist of stable and unstable branches. An equilibrium point $(\underline{X}_0; \underline{m}_0)$ where a locus bifurcates into stable and unstable branches is called a

bifurcation point. In general, it may be one of the following two types: a static or a dynamic (Hopf) bifurcation. It is a static bifurcation (i.e., saddle-node, or transcritical, or pitchfork bifurcation) if the Jacobian matrix $\underline{J}(\underline{X}_0; \underline{m}_0)$ has a zero eigenvalue while all of its other eigenvalues have nonzero real parts. It is a Hopf bifurcation if

- 1) $\underline{F}(\underline{X}_0; \underline{m}_0) = \underline{0}$,
- 2) $\underline{J}(\underline{X}_0; \underline{m}_0)$ has a single pair of complex conjugate eigenvalues, $\underline{s} + j\underline{w}$, whose real part \underline{s} is zero while all of the other eigenvalues have nonzero negative real parts;
- 3) $d\underline{s}/d\underline{m} \neq 0$ at \underline{m}_0 .

The first two conditions imply that the equilibrium point is nonhyperbolic, while the third condition implies a transversal (i.e., a nonzero speed) crossing of the imaginary axis of these eigenvalues. Hence, it is termed a transversality condition. When all of the above three conditions are satisfied, a limit cycle is born at $(\underline{X}_0; \underline{m}_0)$.

2.2 Normal Form Near a Hopf Bifurcation

To derive the equation governing the amplitude a of a limit cycle near a Hopf bifurcation point, $\underline{m} = H$, we seek the normal form of (1) by means of the method of multiple scales [12, 13]. This method allows us to separate the slow- from the fast-varying oscillations. To this end, we let

$$\underline{X} - \underline{X}_0 = \varepsilon \underline{y} \quad \text{and} \quad \underline{m} - H = \varepsilon^2 \underline{m}_2, \quad (3)$$

where \underline{X}_0 is the operating condition at $\underline{m} = H$ and ε is a small dimensionless parameter that allows us to make a time-scale decomposition. Substituting (3) into (1), using Taylor series to expand the result for small ε , and using the fact that $\underline{F}(\underline{X}_0; \underline{m}_0) = \underline{0}$ we obtain

$$\dot{\underline{y}} = \underline{J} \underline{y} + \varepsilon \underline{b}(\underline{y}, \underline{y}) + \varepsilon^2 \underline{c}(\underline{y}, \underline{y}, \underline{y}) + \varepsilon^2 \underline{m}_2 \underline{D} \underline{y} + \dots \quad (4)$$

In (4), \underline{D} is a $n \times n$ constant matrix, $\underline{b}(\underline{y}, \underline{y})$ is generated by a vector-valued symmetric bilinear form and $\underline{c}(\underline{y}, \underline{y}, \underline{y})$ is generated by a vector-valued symmetric trilinear form. For example, an entry of $\underline{b}(\underline{y}, \underline{y})$ is $\underline{y}^T \underline{B} \underline{y}$, where \underline{B} is a constant matrix. At $\underline{m} = \underline{m}_0$, the Jacobian matrix \underline{J} has a pair of purely imaginary eigenvalues $\pm j\underline{w}$, with all the remaining eigenvalues being in the open left-half of the complex plane. Let $T_0 = t$ and $T_2 = \varepsilon^2 t$ be the fast and slow time scales, respectively.

Using the method of multiple scales, we seek a third-order expansion written as

$$\underline{y}(t; \varepsilon) = \underline{y}_1(T_0, T_2) + \varepsilon \underline{y}_2(T_0, T_2) + \varepsilon^2 \underline{y}_3(T_0, T_2) + \dots \quad (5)$$

Substituting (5) into (4) and equating coefficients of like powers of \mathbf{e} yields three equations of orders \mathbf{e} , \mathbf{e}^2 , and \mathbf{e}^3 .

The solution for the equation of order \mathbf{e} is given by

$$\underline{y}_1 = A \underline{p} e^{j\mathbf{w}T_0} + A^* \underline{p}^* e^{-j\mathbf{w}T_0}, \quad (6)$$

while that of order \mathbf{e}^2 is found as

$$\underline{y}_2 = 2 \underline{z}_0 A A^* + 2 \underline{z}_2 A^2 e^{2j\mathbf{w}T_0} + cc. \quad (7)$$

In (7), cc stands for the complex conjugate of the preceding terms. The vectors \underline{z}_0 and \underline{z}_2 are solutions to the algebraic systems of equations given by

$$\underline{J} \underline{z}_0 = -\frac{1}{2} \underline{b}(\underline{p}, \underline{p}), \quad (8)$$

$$\text{and } (2j\mathbf{w}\underline{I} - \underline{J}) \underline{z}_2 = \frac{1}{2} \underline{b}(\underline{p}, \underline{p}). \quad (9)$$

Substituting (6) and (7) into the equation of order \mathbf{e}^3 and eliminating the terms that diverge as time tends to infinity, known as the secular terms, we obtain

$$\underline{\dot{A}} = \mathbf{m}(\mathbf{b}_1 + j\mathbf{b}_3) + 4(\mathbf{b}_2 + j\mathbf{b}_4) \underline{A}^2 \underline{A}^*, \quad (10)$$

where $\mathbf{b}_1 + j\mathbf{b}_3 = \underline{q}^T \underline{D} \underline{p}$,

$$\begin{aligned} \mathbf{b}_2 + \mathbf{b}_4 = & 2 \underline{q}^T \underline{b}(\underline{p}, z_0) + \underline{q}^T \underline{b}(\underline{p}^*, z_2) \\ & + \underline{q}^T \underline{c}(\underline{p}, \underline{p}, \underline{p}^*) \end{aligned}$$

Here, \underline{q} is the left eigenvector of \underline{J} corresponding to the eigenvalue $j\mathbf{w}$. It is normalized so that $\underline{q}^T \underline{p} = 1$.

Substituting $A = (1/2) a e^{j\mathbf{t}}$ into (10) and taking the real part yields the equation governing the amplitude a of the limit cycles for \mathbf{m} near H , which is written as

$$\dot{a} = (\mathbf{m} - H) \mathbf{b}_1 a + \mathbf{b}_2 a^3. \quad (11)$$

The equilibrium point satisfying $\dot{a} = 0$ is given by

$$a = \pm I \sqrt{(\mathbf{m} - H)}, \quad (12)$$

where $I = \sqrt{-\mathbf{b}_1 / \mathbf{b}_2}$. If $\mathbf{b}_2 < 0$, the limit cycle born at $\mathbf{m} = H$ is stable and its amplitude a will grow smoothly from small to large values as \mathbf{m} moves from H into the unstable region. If $\mathbf{b}_2 > 0$, the limit cycle at H is unstable and as \mathbf{m} moves into the unstable region, the system response will jump to a far away response, which may be static or dynamic. In the former case, the Hopf bifurcation point is termed supercritical, while in the latter case it is called subcritical.

Due to the expansion (5), this analysis is valid only in the close neighborhood of H . To study the stability of the limit cycle for values of \mathbf{m} further in the unstable region, we resort to Floquet theory. It will be examined next.

2.3 Floquet Theory

Consider a limit cycle of period T defined as $\underline{X}(t) = \underline{X}(t + T)$. Its stability is analyzed as follows. First, we substitute $\underline{X}(t) = \underline{X}_0(t) + \underline{u}(t)$ into (1). Then, we linearize the obtained equation in $\underline{u}(t)$ to get

$$\dot{\underline{u}} = \underline{J}(X_0; \mathbf{m}) \underline{u}. \quad (13)$$

Finally, we solve the linear system of (13) to determine n linearly independent solutions, $\{\underline{u}_1, \underline{u}_2, \dots, \underline{u}_n\}$, and form the fundamental matrix $\underline{U}(t) = [\underline{u}_1, \underline{u}_2, \dots, \underline{u}_n]$. Usually, one chooses the initial conditions such that $\underline{U}(0) = \underline{I}$, where \underline{I} is the $n \times n$ identity matrix. The stability of $\underline{X}(t)$ is ascertained from the eigenvalues $\{\mathbf{r}_1, \mathbf{r}_2, \dots, \mathbf{r}_n\}$ of $\underline{U}(T)$, known as the monodromy matrix. These eigenvalues are called the Floquet multipliers. One of them is always unity for an autonomous system. If all of the other multipliers are inside the unit circle in the complex plane, the limit cycle is asymptotically stable.

3-TURBINE-GENERATOR MODEL WITH AVR

The foregoing bifurcation analysis is applied to a series-compensated single-machine-infinite-busbar power system that represents characteristics of the CHOLLA # 4 turbine-generator system with respect to the SOWARO station at the Arizona Public Service Company. The generator is provided with a static excitation system known as General Electric Static Excitation or GENERREX for short. Its model has been provided to us by Agrawal and Demcko [15]. The complete set of equations that describe the dynamics of this system is given in [14].

The test data of the d- and q-axes mutual flux linkages, \mathbf{y}_{md} and \mathbf{y}_{mq} , versus the currents, i_d , i_q , i_f , and i_Q , are represented by third-order polynomial functions. The flux linkages \mathbf{y}_d and \mathbf{y}_q can be determined from \mathbf{y}_{md} and \mathbf{y}_{mq} as derived in [16]. The mechanical system consists of high- and low-pressure turbine sections, a generator, and two coupling masses. One mass couples the high-pressure turbine with the low-pressure turbine and the second mass couples the low-pressure turbine with the generator mass. The electrical subsystem consists of damper windings and an AVR.

The turbine-generator system dynamics is governed by 19 first-order differential equations [14]. A pseudo-arclength continuation scheme is used to calculate the equilibrium points as a function of the compensation level \mathbf{m} . It is defined as the absolute ratio evaluated at 60 Hz of the capacitor reactance to the inductance reactance of the transmission line. The 19×19 Jacobian matrix \underline{J} has five real eigenvalues, which are negative and correspond to the AVR, field and damper windings, and 7 pairs of complex conjugate eigenvalues, yielding 7 modes of oscillation.

Two of them are associated with the electrical system and 5 with the mechanical system. The mechanical mode with the lowest frequency of 2.1 Hz is the one usually considered in power-system stability analysis. It is called the swing or electro-mechanical mode since the turbine sections, generator, and exciter oscillate together as a rigid body. As for the other 4 mechanical modes, they are called torsional modes to indicate that some of the shaft masses oscillate against the others. For instance, let us consider the first and second torsional modes. They are of special interest because, under certain conditions described below, they may be self-excited when they interact with one of the electrical modes.

The first torsional mode has a natural frequency of 24.4 Hz and one polarity reversal located between the first mass coupling turbine section and the generator. The second torsional mode has a natural frequency of 31.7 Hz and two polarity reversals, one between the high-pressure turbine and the second mass coupling section.

To study how these oscillatory modes interact with each other, let us analyze variations of the real and imaginary parts of the eigenvalues with the compensation level m which are displayed in Fig. 1. They have been calculated for the generator real and reactive electric powers given by $P_e = 0.9$ pu, $Q_e = 0.4358$ pu and for the generator terminal voltage given by $V_t = 1.0$ pu. For small m the frequencies of the electrical modes are approximately 377 rad/sec, but as m increases, they separate from each other. One of them increases and is called supersynchronous and the other one decreases and is called subsynchronous. This separation of the electric modes occurs because of the exchange of energy that takes place between the series capacitor and the series inductors of the line and of the generator. In this paper, we are interested in the subsynchronous frequency and how its associated mode interacts with the torsional modes. We observe from Fig. 1 (bottom) that the sign of the real part of the eigenvalue of the second torsional mode changes from negative to positive at $m = H \approx 0.819$. As seen in Fig. 1 (top), this change occurs when the frequency of the subsynchronous electrical mode is sufficiently close to that of the second torsional mode. This implies that the influence of the electrical mode on the second torsional mode acquires sufficient strength to move its eigenvalues transversely across the imaginary axis into the right-half of the complex plane at the Hopf bifurcation point, H . At this point, the second torsional mode loses stability. The loci of the machine rotor angle d_r versus m is displayed in Fig. 2. In this figure, the stable branch of the loci is represented by a solid line while the unstable branch is represented by a dashed line. We use the multiple-scales algorithm outlined in Section 2.2 and encoded in Mathematica [17]. For the case depicted in Fig. 2, variation of the

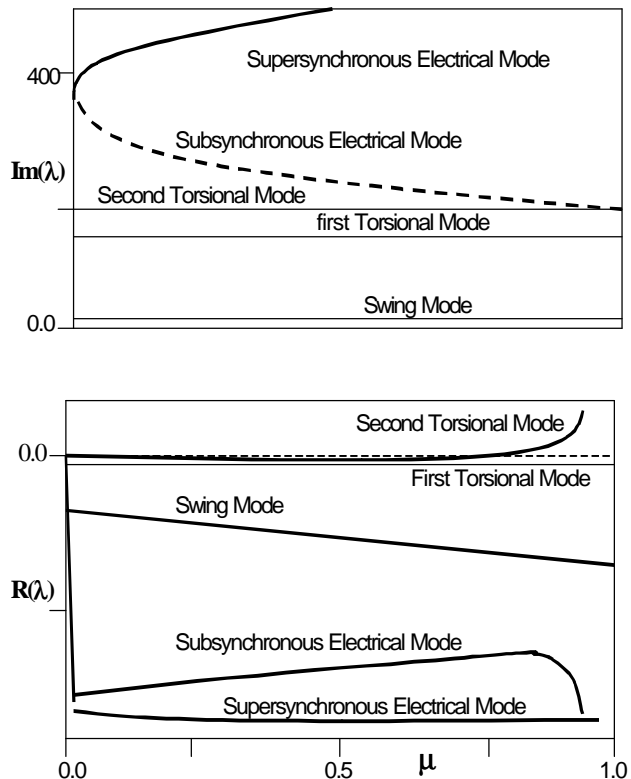


Fig. 1: Variation of the real part (bottom) and imaginary part (top) of the eigenvalues with m for $P_e = 0.9$ and $Q_e = 0.4358$ (without PSS).

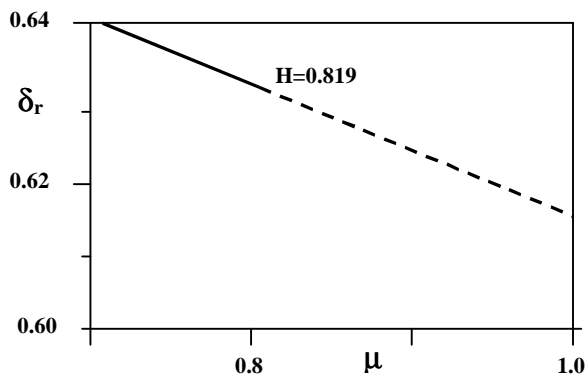


Fig. 2: Variation of the rotor angle d_r (in rad.) with m .

amplitude a of oscillations with time near H is given by (12) with $b_1 = 0.5234$ and $b_2 = -0.00062$, yielding $\lambda = 28.98$. Because $b_2 < 0$, the Hopf bifurcation point $H = 0.819$ is supercritical, yielding stable limit cycles.

For the sake of comparison, let us apply the bifurcation analysis to the turbine-generator model without AVR. In this case, we found that the Hopf bifurcation occurs at a larger value of m specifically at $H = 0.842$. Therefore, we conclude that AVR destabilizes the system because it decreases the stability region. To expand this region, we add a stabilizing signal provided by a PSS as described next.

4 - DESIGN OF A STABILIZER

As shown in [11], the PSS consists of a high-frequency filter and two stages of lead-lag compensation. A simple saturation function limits the amplitude of the output voltage that is added to the terminal voltage error signal. The PSS is governed by a second-order ordinary-differential equation and three first-order ordinary-differential equations given as

$$y_1 + A_1 \ddot{y}_1 + A_2 \dot{y}_1 = V_{S1}, \quad (14)$$

$$y_2 + T_2 \dot{y}_2 = y_1 + T_1 \dot{y}_1, \quad (15)$$

$$y_3 + T_4 \dot{y}_3 = y_2 + T_3 \dot{y}_2, \quad (16)$$

$$V_S + T_5 \dot{V}_S = K_S T_5 \dot{y}_3. \quad (17)$$

Here, A_1 and A_2 are the high-frequency filter constants, V_{S1} is the PSS input, T_1 and T_3 are the lead compensating time constants, T_2 and T_4 are the lag compensating time constants, T_5 is the washout time constant, and K_S is the gain. In this study, the parameter values are set to $A_1 = 0.061$, $A_2 = 0.0017$, $T_1 = 0.3$, $T_2 = 0.03$, $T_3 = 0.3$, $T_4 = 0.03$, $T_5 = 10.0$, $K_S = 5.0$, $V_{SMAX} = 0.05$, $V_{SMIN} = -0.05$, and $K = 0$.

The dynamics of the system with AVR and PSS consists of 24 first-order nonlinear ordinary-differential equations among which 14 represent the electrical subsystem and 10 represent the mechanical subsystem. Again we used a continuation method and found that the Hopf bifurcation occurs at $H \approx 0.8254$. Obviously, this H is shifted to the right compared with the case without PSS analyzed in Appendix A. In other words, the stable region is increased. Variation with time of the amplitude a of the oscillations in the vicinity of H is given by (12) with $\mathbf{b}_1 = 0.533$ and $\mathbf{b}_2 = -0.000035$. Thus, H is supercritical. While the stability region is enlarged thanks to the action of the PSS, the amplitudes of the oscillation in the instability region increase at a faster rate than that without PSS since $\lambda = 128.089$. To circumvent this problem, a nonlinear controller is added to the PSS. It is examined next.

5 - DESIGN OF A NONLINEAR CONTROLLER

A nonlinear controller that reduces the amplitudes of the nonlinear torsional oscillations has been designed using the generator rotor frequency deviation as input signal. To this end, the motion equation of the generator is written as

$$\frac{dw_r}{dt} = \frac{1}{M_5} [-D_5(w_r - 1) + K_{45}(q_4 - d_r) + T_m - T_e] \quad (18)$$

$$\text{where } T_e = i_q Y_d - i_d Y_q \quad (19)$$

$$Y_d = y_{md} - X_{le} i_d \quad (20)$$

$$Y_q = y_{mq} - X_{le} i_q \quad (21)$$

$$y_{md} = d_0 + d_1 (i_f - i_d) + d_2 (i_f - i_d)^2 + d_3 (i_f - i_d)^3 \quad (22)$$

$$y_{mq} = q_0 + q_1 (i_Q - i_q) + q_2 (i_Q - i_q)^2 + q_3 (i_Q - i_q)^3 \quad (23)$$

As seen from the foregoing equations, the nonlinearity is of second order. Because of that, a linear controller would not be very effective in damping the nonlinear torsional oscillations. By contrast, the latter would be suppressed by a nonlinear controller where the frequency deviation, Δw , is squared, multiplied by a gain k , and then injected as an additional feedback loop to the excitation system as $V_{S1} = k \Delta w$. To study the effect of the gain on the performance of the controller, a bifurcation analysis is carried out. For $k = 100$, it is found that variation of the amplitude a of the oscillations with time near $H = 0.8254$ is given by (12) with $\mathbf{b}_1 = 0.573$ and $\mathbf{b}_2 = -0.0025$. Thus, H is still supercritical while the oscillations have much smaller amplitudes since λ has been drastically reduced to 14.93. As k increases, the amplitude a further decreases until it reaches a plateau for k larger than 500. There the improvement becomes insignificant as shown in Fig. 3. Hence, we fix $k = 500$, yielding $\lambda = 6.715$. By further increasing the gain k , one can suppress the secondary Hopf bifurcation and hence the bluesky catastrophe.

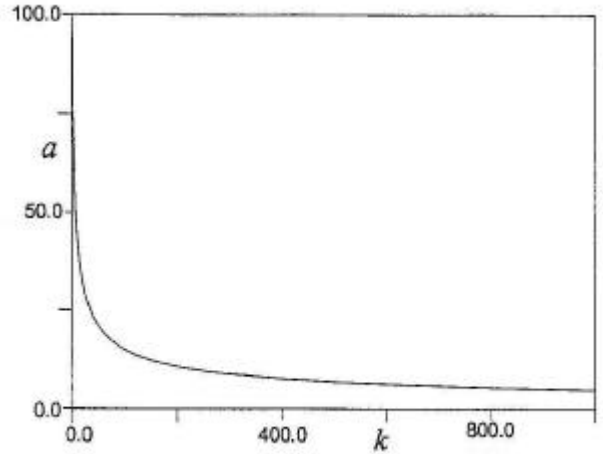


Fig. 3: Variation of a , the amplitude of the limit-cycle born at H , with the nonlinear controller gain k .

6 - CONCLUSIONS

We have applied a bifurcation analysis together with the method of multiple scales and Floquet theory to the CHOLLA # 4 turbine-generator system. We used a complete model that includes the generator damper windings, the generator saturation, and the automatic voltage regulator. The results show that the system loses stability through a Hopf bifurcation, beyond which torsional oscillations start to grow. Studies have also revealed that the AVR reduces the level of compensation that can be used. To increase

this level while significantly damping the torsional oscillations, a PSS and a nonlinear controller have been added to the AVR system.

ACKNOWLEDGEMENTS

The authors would like to thank Drs. B. Agrawal and J. Demcko of the Arizona Public Service Company for providing the excitation model of CHOLLA # 4. Partial financial support provided by NSF under grant ECS-9257204 is gratefully acknowledged.

REFERENCES

- [1] R. G. Farmer, E. Katz, and A. L. Schwalb, "Navajo Project on Subsynchronous Resonance Analysis and Solutions," *IEEE Transactions on Power Apparatus and Systems*, Vol. PAS-96, pp. 1226-1232, July/Aug. 1977.
- [2] IEEE Committee Report, "First Benchmark Model for Computer Simulation of Subsynchronous Resonance," *IEEE Trans. on Power Apparatus and Systems*, Vol. PAS-96, pp. 1565-1570, Sept./Oct. 1977.
- [3] P. M. Anderson, B. L. Agrawal, and J. E. Van Ness. *Subsynchronous Resonance in Power Systems*. IEEE Press, 1990.
- [4] D. N. Walker, C. E. Bowler, R. L. Jackson, and D. A. Hodges, "Results of Subsynchronous Resonance Test at Mohave," *IEEE Trans. on Power Apparatus and Systems*, Vol. PAS-94, pp. 1878-1889, Sep./Oct. 1975.
- [5] N. G. Hingorani, "A New Scheme for Subsynchronous Resonance Damping of Torsional Oscillations and Transient Torque – Part I," *IEEE Trans. on Power Apparatus and Systems*, pp. 1852-1857, April 1981.
- [6] M. R. Iravani and A. Semlyen, "Hopf Bifurcations in Torsional Dynamics (Turbine-Generators)," *IEEE Trans. on Power Systems*, Vol. PAS-7, pp. 28-36, Feb. 1992.
- [7] A. H. Nayfeh and B. Balachandran. *Applied Nonlinear Dynamics*. Wiley-Interscience, 1995.
- [8] Y. Mitani, K. Tsuji, M. Varghese, F. F. Wu, and P. Varaiya, "Bifurcations Associated with Sub-Synchronous Resonance," *IEEE Trans. on Power Systems*, Vol. 13, No. 1, pp. 139-144, Feb. 1998.
- [9] W. Zhu, R. R. Mohler, R. Spee, W. A. Mittelstadt, and D. Maratukulam, "Hopf Bifurcation in a SMIB Power System with SSR," *IEEE Trans. on Power Systems*, Vol. 11, No. 3, pp. 1579-1584, Aug. 1996.
- [10] A. H. Nayfeh, A. M. Harb, C.-M. Chin, A. M. A. Hamdan, and L. Mili, "A Bifurcation Analysis of Subsynchronous Oscillations in Power Systems," *Electric Power Systems Research*, Vol. 47, pp. 21-28, 1998.

- [11] A. H. Nayfeh, A. M. Harb, C. - M. Chin, A. M. A. Hamdan, and L. Mili, "Application of Bifurcation Theory to Subsynchronous Resonance in Power Systems," *International Journal of Bifurcation and Chaos*, Vol. 8, No. 1, pp. 157-172, 1998.
- [12] A. H. Nayfeh. *Perturbation Method*. Wiley-Interscience, 1973.
- [13] A. H. Nayfeh. *Introduction to Perturbation Techniques*. Wiley-Interscience, 1981.
- [14] A. M. Harb. *Application of Bifurcation Theory to Subsynchronous Resonance in Power Systems*. Ph.D. Thesis, Virginia Tech, Dec. 1996
- [15] B. Agrawal and J. Demcko, Personal Communication, Arizona Public Service.
- [16] P. Kundur. *Power System Stability and Control*. McGraw-Hill, 1994.
- [17] A. H. Nayfeh and C. M. Chin. *Perturbation Methods with Mathematica*. Dynamic Press, 1999.

APPENDIX: GENERATOR WITHOUT AVR

When the bifurcation analysis is applied to the turbine-generator model without AVR, the Hopf bifurcation occurs at $H = 0.842$. At this point, a stable limit cycle is born; its time-trace and phase portrait are displayed in Fig. 4 (a). When m increases beyond H , the amplitude of the limit cycle increases until it starts to modulate past a critical value, $m = SH \approx 0.84665$, called secondary Hopf bifurcation [7]. There, two of the Floquet multipliers exit the unit circle away from the real axis and the limit cycle gives way to a two-period quasiperiodic (two-torus) attractor as displayed in Fig. 4 (b) and 4 (c). The corresponding time traces depicted in Fig. 4 (right) suggest that the oscillations have two incommensurate periods. The FFT of δ_t consists of two incommensurate frequencies, their multiples, and combinations. As m increases slightly above $SH \approx 0.89765$, the two-torus shown in Fig. 4 (c) collides with its basin boundary, resulting in their destruction, in a so-called bluesky catastrophe [7]. The latter is displayed in Fig. 5.

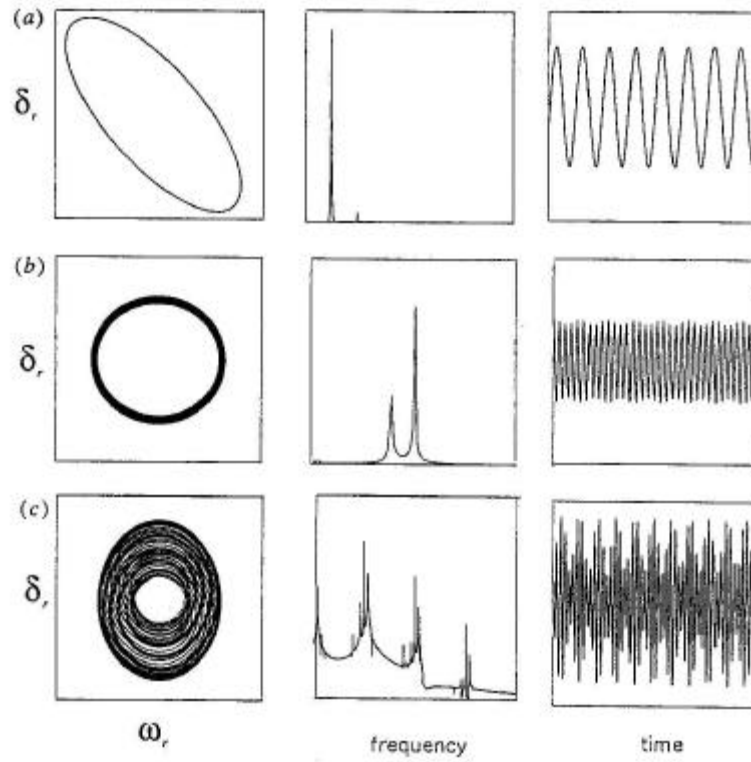


Fig. 4: Two-dimensional projections of the phase portrait onto the w_r - d_r plane (left), the FFT of the corresponding generator rotor angle d_r (middle), and the time traces of the d_r (right) at $m =$ (a) 0.842351, (b) 0.848651, and (c) 0.887651. The solution at (a) is a limit cycle, at (b) is a two-torus attractor recorded well before the bluesky catastrophe, and at (c) is a two-torus attractor located just before it disappears in a bluesky catastrophe.

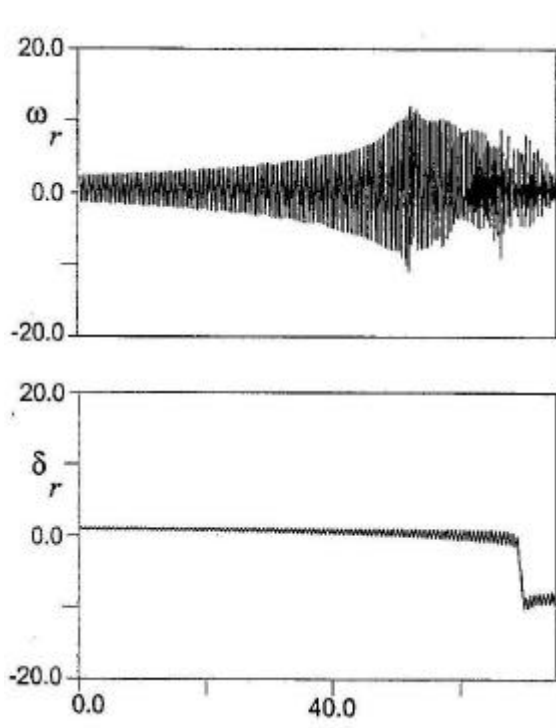


Fig. 5: Time histories of the generator rotor speed w_r (in rad/sec) and angle d_r (in rad) in the vicinity of the bluesky catastrophe that occurs at $C \approx 0.8976$.